Imaging of Primary Posterior Fossa Brain Tumors in Children

William T. O'Brien, Sr., D.O.

Department of Radiology, Wilford Hall Ambulatory Surgical Center, Joint Base San Antonio-Lackland, TX
Department of Radiology, Uniformed Services University of the Health Sciences, Bethesda, MD

Introduction

Brain tumors represent the most common solid neoplasm in children and second most common pediatric malignancy overall, following leukemia. Outside of infancy, the majority of primary childhood brain tumors occur in the infratentorial compartment and include medulloblastoma, juvenile pilocytic astrocytoma (JPA), ependymoma, and brainstem/ pontine glioma; atypical teratoid rhabdoid tumor (ATRT) is an additional rare but important primary brain tumor of early childhood.

Children with posterior fossa brain tumors typically present with signs and symptoms related to increased intracranial pressure, gait disturbances, and/or cranial nerve deficits, depending upon the type, size, and location of the tumor. CT and MR evaluation is critical in the work-up, management, and follow-up of these patients. This article aims to provide an overview of the imaging manifestations and appearances of the most common primary posterior fossa brain tumors in children.

Medulloblastoma

Background.

Medulloblastoma is a highly malignant (grade IV) embryonal cerebellar tumor which occurs most frequently in children but may also affect adults. It is the second most common pediatric brain tumor overall, following astrocytoma, but is the most common pediatric posterior fossa tumor, accounting for up to 40% of cases.[1-5] In the pediatric population, there are two age peaks – one at 3 and one at 7 years of age;[6] in adults, the peak age of presentation is between 20 and 40 years of age.[3,7,8] Boys are affected more often than girls by a ratio of greater than 2:1. There is an association and increased incidence in the setting of basal cell nevus, or Gorlin, syndrome.

Medulloblastomas are categorized into various pathologic subtypes, including classic, desmoplastic, extensively nodular, large cell, and anaplastic.[3,9] The classic subtype is by far the most common. An additional rare subtype is the melanotic medulloblastoma, which appears similar to a classic medulloblastoma on imaging but has melanotic tint on gross inspection. The vast majority of medulloblastomas (85-90%) arise from the midline cerebellar vermis dorsal to the fourth ventricle.[10] Approximately 10-15% occur within the cerebellar hemispheres, which is more common in older patients with the desmoplastic variant.[1] More aggressive variants may be infiltrative and invade the fourth ventricle and adjacent brainstem or cerebellar parenchyma.

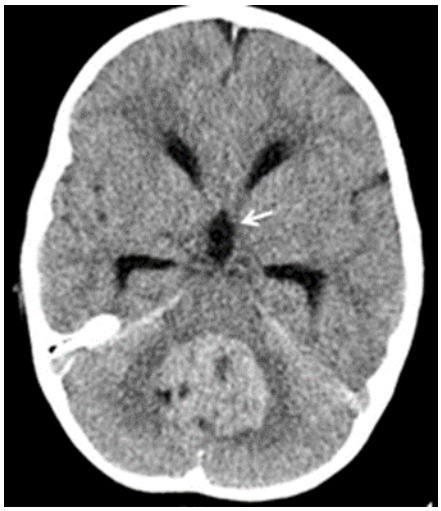

Figure 1. Medulloblastoma. Unenhanced axial CT image reveals a well-circumscribed midline hyperdense posterior fossa mass with small hypodense cystic regions. There is compression of the 4th ventricle with obstructive hydrocephalus, as evidenced by enlargement of the third (arrow) and visualized portions of the lateral ventricles.

Children with medulloblastomas most often present clinically with a relatively rapid onset of symptoms - over the course of weeks or a few months - due to the rapid growth and malignant features of the neoplasm. The most common symptoms include headaches and nausea/vomiting due to obstructive hydrocephalus; truncal ataxia and papilledema are common clinical findings. Tumoral seeding of the cerebral spinal fluid (CSF) is present in approximately one-third of cases at the time of initial diagnosis.

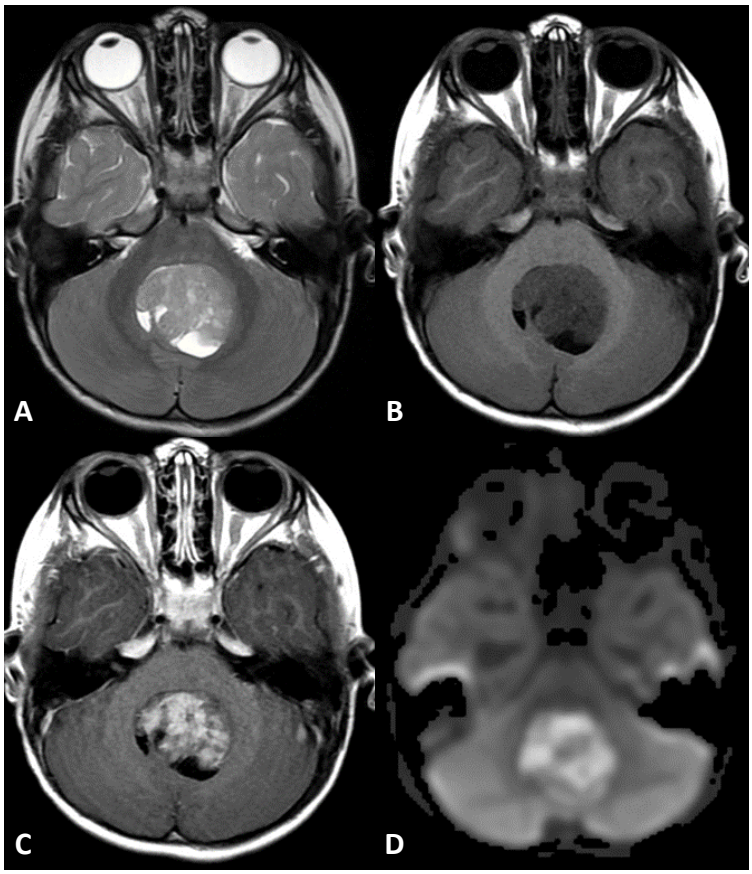

Figure 2. Medulloblastoma. Axial T2 MR image (**A**) demonstrates a well-circumscribed, midline posterior fossa mass which is hyperintense compared to white matter and iso- to slightly hyperintense compared to gray matter with small cystic components. The mass is hypointense on T1 (**B**) with avid enhancement of solid components (**C**). Diffusion-weighted image (DWI) shows characteristic increased signal (**D**). ADC map (not shown) demonstrated corresponding hypointensity. The mass compresses the 4th ventricle.

Imaging Findings.

On CT, medulloblastomas typically present as well-defined, midline posterior fossa masses. The high cellularity with increased nuclear-to-cytoplasmic ratio leads to increased attenuation on unenhanced CT in approximately 90% of cases (**Fig. 1**); the remainder are isodense to brain parenchyma.[3] Surrounding parenchymal vasogenic edema is noted in >90% of cases. After contrast administration, there is often avid enhancement which may be homogeneous or heterogeneous. Calcifications are seen in approximately 20% of cases; cysts are more common and occur in 50-60% of cases.[11] As the lesions grow, there is anterior displacement and compression of the fourth ventricle, which often leads to obstructive hydrocephalus in approximately 90% of cases.[12] If uncompensated, transependymal flow of CSF may be seen along the margins of the lateral ventricles.

On MRI, the majority of medulloblastomas are iso- to hypointense compared to white matter on T1 sequences and variable in signal on T2 sequences.[3] The T2 signal variability has to do with the cellularity of the tumor. More cellular components are hypointense, while less cellular components are iso- to mildly hyperintense compared to white matter. Increased cellularity also leads to increased signal intensity on diffusion weighted sequences; although helpful, this finding has some overlap with other posterior fossa tumors .[13] Medulloblastomas commonly demonstrate avid but heterogeneous enhancement on MRI (**Fig. 2**). Regions of CSF dissemination present with focal (more common) or diffuse leptomeningeal enhancement, which is typically nodular (**Fig. 3**). MR spectroscopy demonstrates a tumoral spectra with increased choline and decreased N-acetyl aspartate (NAA), along with decreased creatine. Lipid-lactate doublets may also be seen. An elevated taurine peak has recently been shown to be a specific MRS finding for medulloblastoma (**Fig. 4**).[14-15]

Medulloblastomas grow in a circumferential pattern and maintain rounded borders. Unlike ependymomas, which are soft and pliable, medulloblastomas infrequently extend through CSF outlet foramina. When aggressive, however, medulloblastomas may be more infiltrative and invade the fourth ventricle, brainstem, and/or adjacent cerebellar parenchyma.

Preoperatively, it is critical to evaluate the entire neuroaxis on MRI to look for disseminated disease (**Fig. 5**). Failure to do so could complicate management decisions. Postoperatively, surveillance imaging of the brain and spine is typically performed at 3-6 months intervals for the first 5 years following initial therapy to evaluate for early recurrence or new CSF dissemination.[3] Although the long-term impact of surveillance imaging on overall survival is debated, early detection of new or recurrent disease may alter clinical management.

Treatment.

Treatment options depend upon the age of the patient and extent of disease and include surgical resection with radiation and/or chemotherapy. Although medulloblastomas are relatively radiation-

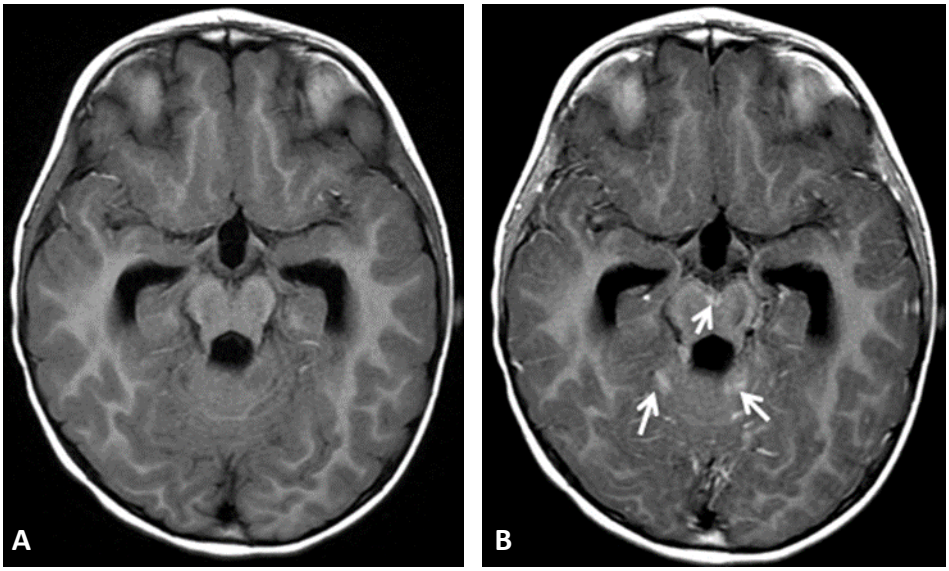

Figure 3. Medulloblastoma CSF Seeding. Pre (**A**) and post (**B**) contrast T1 MR images reveals multiple foci of nodular enhancement along the cerebellar sulci and interpeduncular cistern (arrows). There is also enlargement of the visualized portions of the ventricles due to obstructive hydrocephalus.

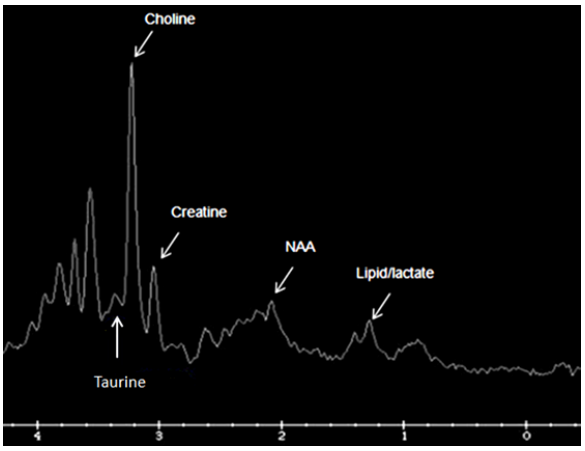

Figure 4. Medulloblastoma. MR spectra reveals elevated choline, decreased NAA, and the presence of a lipid/lactate doublet. A taurine peak is specific for medulloblastoma.

Figure 5. Medulloblastoma CSF Seeding. Sagittal post-contrast T1 image with fat-suppression demonstrates multiple foci of nodular leptomeningeal enhancement along the distal cord, conus, and cauda equina (arrows).

sensitive, radiation therapy is typically avoided prior to 3 years of age due to the potentially devastating effects of craniospinal radiation to the developing CNS. The primary exceptions are in the presence of known CSF dissemination or with tumor recurrences. Neoadjuvant chemotherapy has produced promising results;[16] its use prior to or after surgical resection has allowed for avoidance of craniospinal radiation in many cases of patients under 3 years of age and decreased the overall radiation dose needed to minimize the likelihood of tumor dissemination or recurrence. For children over 3 years of age, craniospinal radiation is typically performed after surgical resection – with or without adjuvant chemotherapy.

Prognosis.

The prognosis for medulloblastoma is based upon age at the time of presentation, presence or absence of CSF dissemination, and residual tumor following initial surgical resection.[17] The best prognosis (approximately 80% 5-year survival) is for children greater than 3 years of age and adults at the time of presentation with no evidence of CSF dissemination and no or minimal residual post-operative disease. The presence of CSF dissemination at the time of diagnosis drops the 5-year survival rate to between approximately 30 and 50%.[18]

Cerebellar Juvenile Pilocytic Astrocytoma (JPA)

Background.

JPAs are low grade neoplasms (WHO grade I) which occur most often in children and young adults. Common locations include the cerebellum, optic pathways, and hypothalamus. Supratentorial hemispheric involvement is more common in adults than children. There is an association and increased incidence of JPAs in the setting of NF-1, particularly involving the optic pathways. JPAs are the most common subtype of pediatric gliomas and account for 85% of all cerebellar astrocytomas;[19] diffuse cerebellar astrocytomas are less common variants. Cerebellar JPAs represent approximately one-third of posterior fossa tumors in children, second in incidence only to medulloblastoma. The peak age of presentation is between 5 and 15 years of age, and boys and girls are affected equally.

Patients with cerebellar JPAs typically present with a gradual onset of symptoms due to slow growth of the tumor. Common presenting symptoms include headache, nausea and vomiting, gait imbalance, and visual disturbances. Common clinical findings include truncal ataxia and papilledema (due to increased intracranial pressure).

Imaging Findings.

Posterior fossa JPAs demonstrate imaging features, such as enhancement patterns and MR spectra, which are incongruent with their biological nature, meaning that some of their imaging features are more often associated with higher grade tumors, rather than a low grade astrocytoma. JPAs may present as midline or off-midline (more common) masses due to vermian or hemispheric involvement, respectively. They are typically well-circumscribed, round or ovoid, and have a large cystic component with a mural nodule. A less common appearance is a solid component peripherally with central necrosis.

On CT, the cystic component is hypodense and the solid nodular component is isodense compared to surrounding brain parenchyma. Adjacent parenchymal edema may occur but is less common due to the indolent nature of JPAs. With contrast administration, there is avid enhancement of the solid nodule and occasionally the walls of the cyst; enhancement of the cyst wall suggests but is not diagnostic of the presence of tumor cells within the cyst wall lining. A less common appearance is solid peripheral enhancement with central necrosis. Larger masses result in compression and obstruction of the fourth ventricle with associated hydrocephalus. If uncompensated, transependymal flow of CSF may be seen along the margins of the lateral ventricles.

On MRI, the cystic component is hypointense on T1 and hyperintense on T2 sequences, similar to CSF signal intensity. The solid components are T1 hypointense and T2 hyperintense compared to surrounding brain parenchyma. Vasogenic edema, when present, is relatively mild compared to the size of the lesion and is T2 hyperintense. After contrast administration, there is avid enhancement of the solid

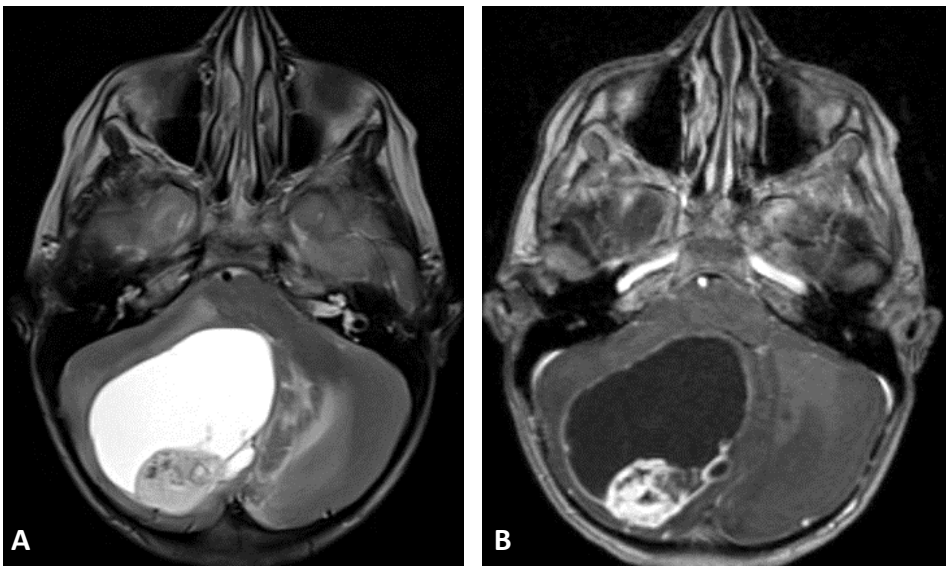

Figure 6. Juvenile Pilocytic Astrocytoma. Axial T2 MR image (**A**) demonstrates a large cystic mass with solid mural nodule centered within the right cerebellar hemisphere. There is surrounding vasogenic edema and compression of the 4th ventricle. Post-contrast T1 image (**B**) reveals avid enhancement of the solid nodule.

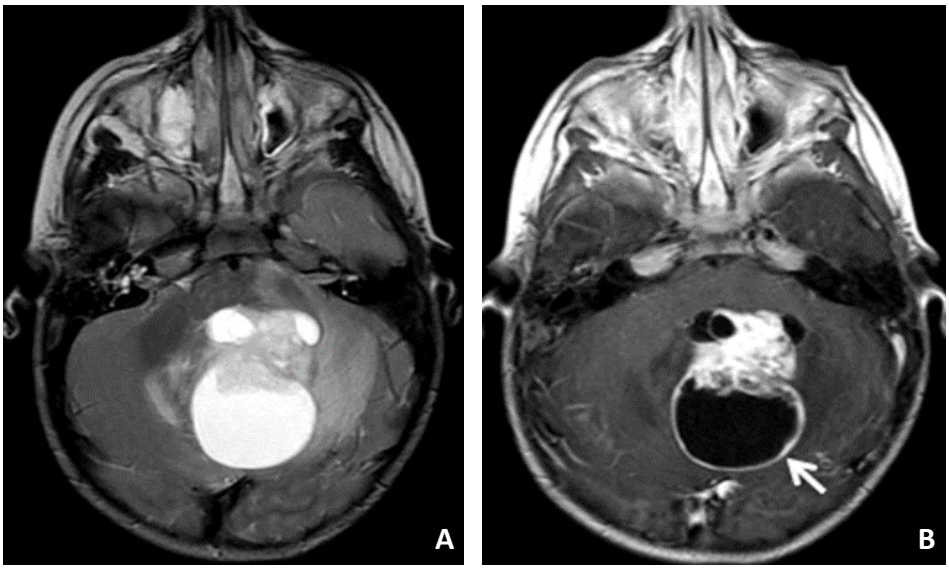

Figure 7. Juvenile Pilocytic Astrocytoma. Axial T2 MR image (**A**) demonstrates a large cystic mass with solid mural nodule centered within the posterior fossa. There is surrounding vasogenic edema which extends into the left cerebellar peduncle and brainstem, as well as compression of the 4th ventricle. Post-contrast T1 image (**B**) reveals avid enhancement of the solid nodule, along with enhancement of the cyst wall (arrow), which is suggestive but not diagnostic of tumor cells lining the cyst cavity.

nodular component (**Fig. 6**). As discussed above, enhancement of the cyst wall may occasionally be seen and is suggestive but not diagnostic of tumor cells lining the cyst wall (**Fig. 7**). Rarely, the nodule of a JPA may show increased signal on DWI; however, the high ADC will typically allow differentiation from high grade differentials, such as medulloblastoma.[20] On MR spectroscopy, JPAs have a spectra which may be confused with higher grade tumors – increased choline/creatine due to very low creatine levels, decreased N-acetylaspartate (NAA), decreased myo-inositol, and increased lactate.[21] Obstructive hydrocephalus will lead to ventriculomegaly proximal to the obstruction with transependymal flow of CSF, if uncompensated; the transependymal flow presents as a rind of increased T2 signal intensity along the margins of the lateral ventricles.

Treatment.

Surgical resection of cerebellar astrocytomas is the primary treatment and is considered curative in the setting of gross total resection.[19] Repeat surgical resection is the treatment of choice for recurrences or regrowth after subtotal resection. Radiation and/or chemotherapy is reserved for rare instances of disseminated disease or in cases which are not amenable to surgical resection.[19,22]

Prognosis.

The overall prognosis for cerebellar astrocytomas is excellent and is primarily based upon the lesion location and presence or absence of neurological deficits at the time of presentation. The 10-year survival rate is greater than 90%; complete surgical resection is generally considered curative.

Ependymoma

Background.

Ependymomas arise from ependymal cells which line the ventricles and the central canal of the cord. They may occur at any age but are most common in children and young adults, especially when located within the posterior fossa/fourth ventricle. Approximately 70% of ependymomas are infratentorial,[23] and they are the third most common pediatric posterior fossa tumor, following medulloblastoma and cerebellar juvenile pilocytic astrocytoma. They occur along the floor (more common) or roof of the fourth ventricle. The mean age of presentation for infratentorial ependymomas is 6 years of age,[24] and there is a slight male predominance. Supratentorial intraventricular and intraparenchymal (extraventricular) ependymomas are more common in adults.

The majority of ependymomas are WHO grade II tumors; a more aggressive anaplastic variant is less common. Ependymomas are soft, pliable tumors which have a propensity for spread through ventricular outlet foramina, which is fairly characteristic. CSF dissemination at initial presentation is estimated in approximately 12% of cases and is more common with

more aggressive histology.[23,25]

Children with ependymomas most often present clinically with symptoms related to increased intracranial pressure due to hydrocephalus; the most common symptoms include headaches, nausea/ vomiting, and gait imbalance; truncal ataxia and papilledema are the most common clinical findings.

Imaging Findings.

On CT, posterior fossa ependymomas appear as fourth ventricular masses with solid components which are typically isodense to mildly hyperdense compared to surrounding brain parenchyma.[23] Lesions result in obstructive hydrocephalus with nausea and vomiting in roughly 90% of patients.[23,26] If uncompensated, transependymal flow of CSF may be seen along the margins of the lateral ventricles. Compared to medulloblastoma, ependymomas are more heterogeneous; calcifications are noted in roughly 50% of cases, cysts in approximately 20% of cases, and hemorrhage in 10% of cases.[23] Solid components avidly but heterogeneously enhance. Ependymomas are soft and pliable, insinuating along tissue margins and through foramina; extension through the foramina of Luschka and/or Magendie is highly characteristic, although not pathognomonic. They may also encase surrounding nerves and vessels.

On MRI, posterior fossa ependymomas are iso- to hypointense on T1 and hyperintense on T2 sequences compared to surrounding brain parenchyma and demonstrate heterogeneous enhancement of solid components (**Fig. 8**). Signal characteristics of solid components are more heterogeneous compared to medulloblastoma, especially with foci of calcification, hemorrhage, or cystic change. More cellular components of ependymomas may show increased signal on DWI sequences; ADC maps are typically intermediate in signal with some overlap compared to medulloblastomas.[20] Ependymomas fill and obstruct the fourth ventricle as they growth, often resulting in hydrocephalus. Extension through fourth ventricular outlet foramina and encasement of surrounding structures is better depicted on MRI compared to CT (**Figs. 9 and 10**). MR spectroscopy often reveals a nonspecific tumor spectra with elevated choline and decreased N-acetylaspartate (NAA).[23]

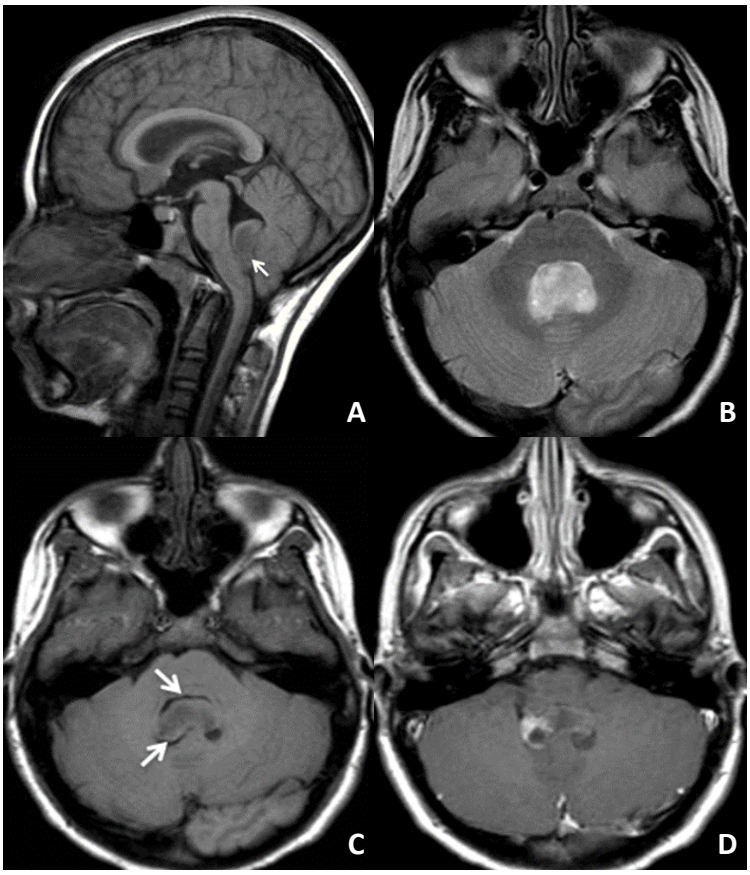

Figure 8. Ependymoma. Sagittal T1 MR image (**A**) reveals an iso- to hypointense mass centered within the inferior aspect of the 4th ventricle (arrow). Axial images show that the mass is hyperintense on T2 (**B**) and hypointense on T1 (**C**) sequences with heterogeneous enhancement of the solid components (**D**). CSF within the 4th ventricle is seen surrounding the mass (C – arrows).

Figure 9. Ependymoma Foraminal Extension. Sagittal T1 MR image reveals an iso- to hypointense mass centered within the inferior 4th ventricle with extension through the foramen magnum and along the dorsal aspect of the upper cervical cord (arrow).

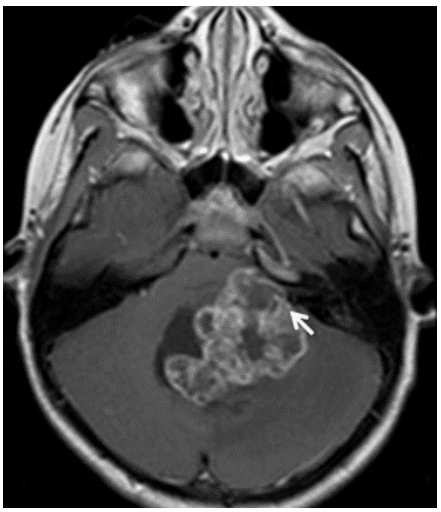

Figure 10.
Ependymoma Foraminal Extension.
Axial post-contrast T1 MR image reveals a lobulated, heterogeneously enhancing posterior fossa mass centered within the 4th ventricle with extension into the left cerebellopontine angle (arrow).

Figure 11.
Ependymoma CSF Seeding.
Sagittal post-contrast T1 image with fat-suppression demonstrates a nodular region of abnormal enhancement along the cauda equina (arrow).

Foci of CSF dissemination are best seen on post-contrast sequences as regions of leptomeningeal enhancement, which is most often nodular and located along the cerebellar sulci and spinal canal (**Fig. 11**); pre-operative evaluation of the spine to evaluate for drop metastases is important for both management and post-operative follow-up. Postoperatively, surveillance imaging of the brain and spine is typically performed to evaluate for recurrence or new CSF dissemination.

Treatment.

Surgical resection is the primary treatment of choice. Complete resection is difficult due to tumor pliability and adherence to adjacent structures; thus, recurrence is common. Post-operative radiation therapy is performed in the surgical bed with craniospinal radiation for disseminated disease or drop metastases, although radiation therapy is typically avoided prior to 3 years of age due to the potentially devastating effects of craniospinal radiation to the developing CNS.

Prognosis.

The prognosis of posterior fossa ependymoma is primarily based upon the degree of initial surgical resection and presence or absence of disseminated or recurrent disease. The overall 5-year survival rate is between roughly 50% and 75%; a younger age at presentation, CSF dissemination, and recurrence correlate with a worse prognosis.[24]

Brainstem/Pontine Glioma

Background.

Brainstem gliomas vary in histology and prognosis based upon location and are fourth in incidence in terms of pediatric posterior fossa tumors, accounting for approximately 15% of cases. There is an equal incidence between boys and girls.[27]

Diffuse intrinsic pontine glioma (DIPG) is the most common and most aggressive subtype of brainstem glioma. The majority are fibrillary astrocytomas (WHO grade II) with focal progression to anaplastic or even glioblastoma multiforme variants. Low-grade variants occasionally occur in the pons but are more common within the medulla and tectal plate; the discussion for this review will focus on the more common DIPG variant.

Children with brainstem gliomas most often present with relatively rapid onset (weeks) of cranial nerve deficits, long tract signs, and occasionally ataxia.[28]

Imaging Findings.

On CT, DIPG presents as diffuse, infiltrative hypodensity with expansion of the pons, often affecting more than 50-75% of the cross-sectional area.[28] The MR appearance is similar with diffuse decreased T1 and increased T2 signal abnormality, which is ill-defined. There is heterogeneous enhancement of the solid components following contrast administration; enhancement characteristics vary during treatment. Cystic or necrotic components

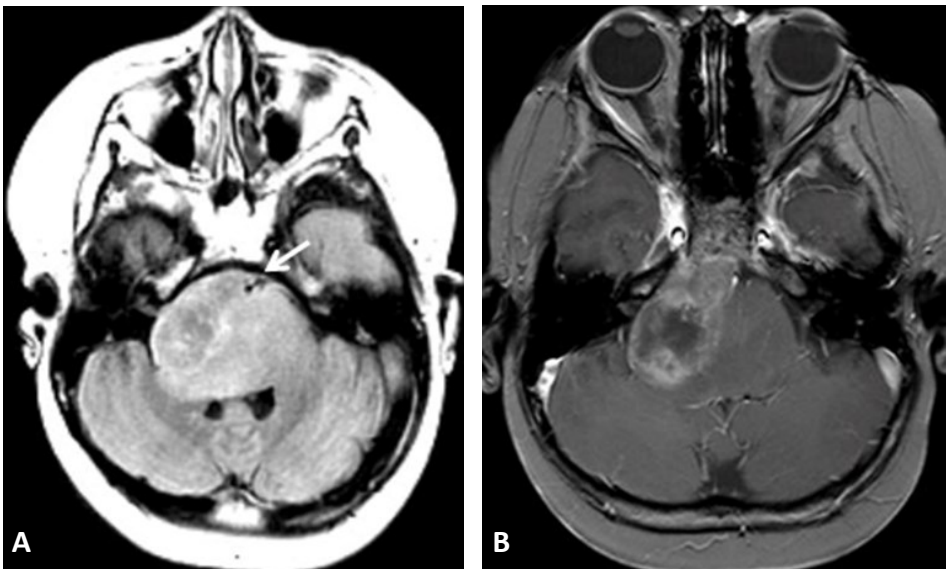

Figure 12. DIPG. Axial FLAIR image (**A**) reveals a hyperintense pontine mass with expansion of the brainstem. Anteriorly, the mass engulfs the basilar artery (arrow), and posteriorly, the mass extends into and compresses the 4th ventricle. Post-contrast T1 image with fat suppression (**B**) shows prominent enhancement with a region of central necrosis posteriorly on the right.

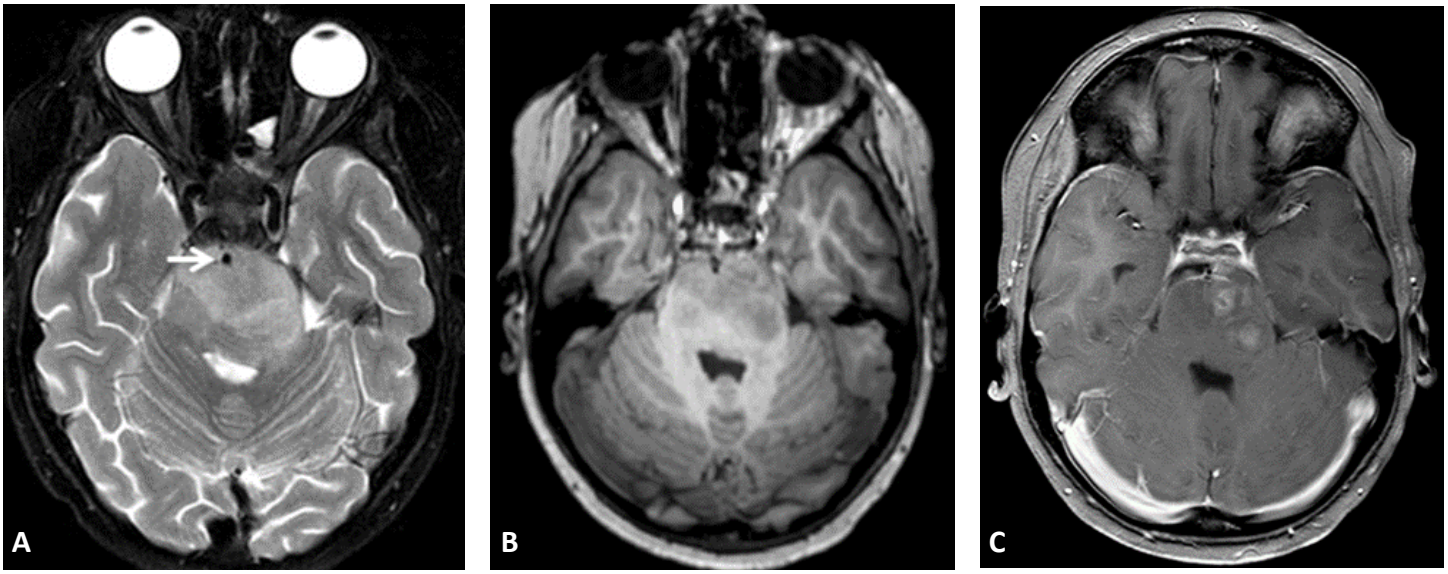

Figure 13. DIPG. Axial T2 MR image (**A**) demonstrates a diffuse, infiltrative T2 hyperintense mass with expansion of the pons. Anteriorly, the mass engulfs the basilar artery (arrow). Posteriorly, the mass projects into the 4th ventricle on the left. Pre (**B**) and post (**C**) contrast T1 images reveal patchy, heterogeneous enhancement.

are not uncommon with higher grade lesions (**Fig. 12**). Perfusion and diffusion-weighted imaging are useful for evaluation of focal progression to a higher grade or to guide biopsy on the rare occasion where the diagnosis is unclear. Regions of increased cellularity will show increased signal on DWI, decreased signal on ADC maps, and increased perfusion. MR spectroscopy shows a tumor spectrum with increased choline and decreased N-acetylaspartate (NAA); the degree of increase (choline) or decrease (NAA) is proportional to the grade of the tumor. Higher grade lesions or regions will also commonly show a lactate peak.

When large, exophytic components of DIPG may be seen anteriorly with engulfment of the basilar artery (**Figs. 12, 13, and 14**) or posteriorly projecting into the fourth ventricle (**Figs. 12, 13, and 14**). Obstruction of the fourth ventricle is typically a late finding. As the tumor progresses, it may extend posteriorly, cephalad, and caudad along white matter tracts (**Fig. 14**).[28]

Treatment.

Due to the critical brainstem location, surgery is not a viable option for the treatment of brainstem gliomas, aside from debulking of exophytic components. Radiation and adjuvant chemotherapy

are the mainstays of treatment in children older than 3 years of age; in children under 3 years of age, attempts are made to minimize or avoid radiation therapy due to its potentially devastating effects to the developing CNS.

Prognosis.

Prognosis for DIPG is dismal with a nearly 100% mortality rate.[29] Median survival is approximately 9-12 months with aggressive treatment.[28]

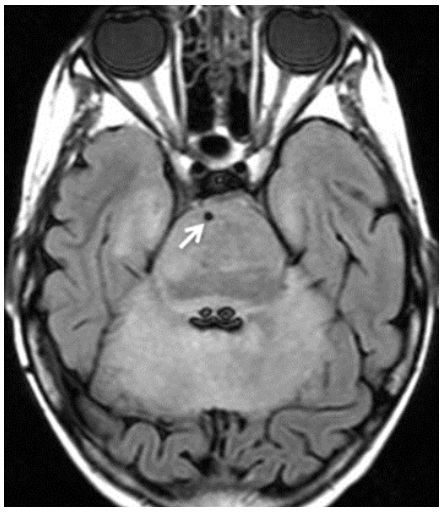

Figure 14. DIPG. Axial FLAIR image reveals a diffuse pontine mass which engulfs the basilar artery anteriorly (arrow) and projects into and compresses the 4th ventricle posteriorly. The mass has extended into the cerebellum and medial aspects of the temporal lobes.

Atypical Teratoid Rhabdoid Tumor (ATRT)

Background.

ATRT is an uncommon, highly malignant tumor which is composed of rhabdoid cells plus primitive neuroectodermal tumor components. It occurs most often in very young children (<3 years of age), although it may occasionally occur in older children and adults. More than half are infratentorial, while the remainder are supratentorial in location.[30,31]

The precise incidence of ATRT is difficult to determine, since it is believed that ATRT is significantly under-diagnosed and misdiagnosed as medulloblastoma, especially in infants and young children.[32,33] If not suspected prospectively, routine histological results will favor medulloblastoma. Therefore, it is important to consider ATRT in the appropriate setting in order to guide the histological evaluation;[33] the presence of rhabdoid cells is a key distinguishing feature from medulloblastoma.

Children with posterior fossa ATRTs present with a rapid onset of symptoms – over the course of days to weeks; headaches and nausea and vomiting are most common. Older children also present with truncal ataxia, while infants present with increase in head size. CSF seeding is common at presentation and may result in multifocal disease.

Imaging Findings.

There is significant overlap in the imaging appearance of posterior fossa ATRT and medulloblastoma; however, some distinguishing features may help suggest ATRT, especially in children under 3 years of age.[34]

On CT, ATRT most often presents as a large, iso- to hyperdense mass which may be midline or off-midline (more common) (**Fig. 15**). A cerebellopontine angle (CPA) location is highly characteristic for ATRT.[33,34] ATRT is more likely to appear heterogeneous compared to medulloblastoma with large eccentric cystic components, visible calcifications, and intratumoral hemorrhage.[33,34] Despite the aggressive features, there is often little or no vasogenic edema within the surrounding parenchyma. Solid components demonstrate avid but heterogeneous enhancement. CSF dissemination may present as regions of leptomeningeal enhancement or multifocal masses with similar imaging characteristics to the primary tumor. Hydrocephalus due to compression and obstruction of the fourth ventricle occurs in approximately 60-65% of cases, which is less frequent than with medulloblastoma.[34] If uncompensated, transependymal flow of CSF may be seen along the margins of the lateral ventricles.

On MRI, ATRTs are typically iso- to hypointense compared to white matter on T1 sequences; however, intratumoral hemorrhage will demonstrate regions of T1 hyperintensity, which are more characteristic of ATRT compared to medulloblastoma. As with medulloblastomas, T2 signal intensity is variable; more cellular components are T2 hypointense, while less cellular components are iso- to mildly hyperintense compared to white matter. Eccentric cysts are commonly seen and are T2 hyperintense. Foci of calcification are hypointense on all sequences and may demonstrate blooming on gradient echo sequences. High cellularity of solid components leads to hyperintensity on DWI, similar to medulloblastoma.

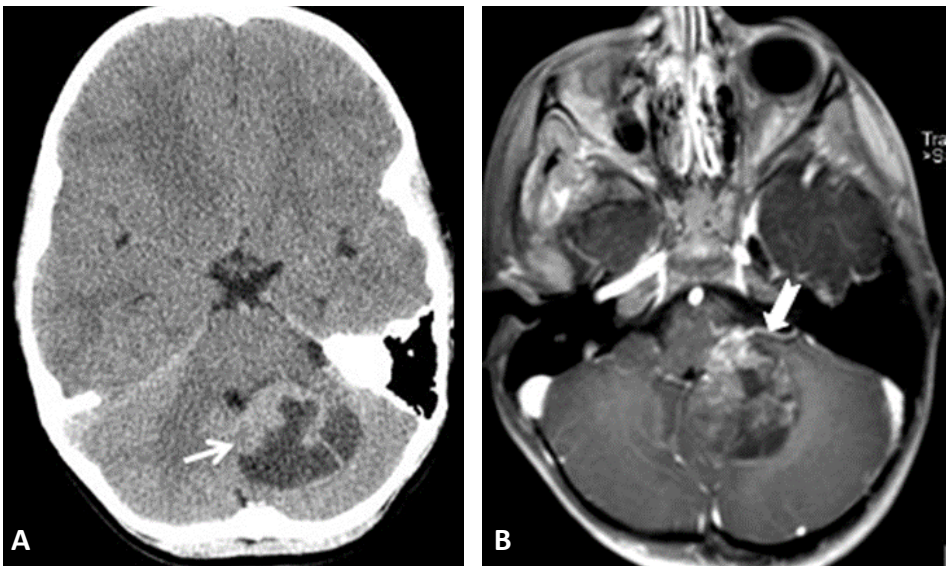

Figure 15. ATRT.
Unenhanced axial CT image (**A**) demonstrates an off-midline slightly hyperdense posterior fossa mass (arrow) with cystic components. There is mass effect on the 4th ventricle. No significant vasogenic edema is seen. Axial post-contrast T1 image with fat suppression (**B**) reveals heterogeneous enhancement of the solid components, as well as extension into outlet foramina and overlying leptomeningeal enhancement (notched arrow).

ATRT demonstrates avid but heterogeneous enhancement of solid components (**Fig. 15**), including the walls of the eccentric tumoral cysts. CSF dissemination may present with foci of leptomeningeal enhancement, which is often nodular, or multifocal masses.

Treatment.

ATRT is aggressive and less responsive to therapeutic options compared to medulloblastoma.[32,34,35] Treatment options are dependent upon patient age and the extent of disease and include surgical resection with radiation and/or adjuvant chemotherapy. Radiation therapy is typically decreased in dosage or avoided prior to 3 years of age due to the potentially devastating effects of craniospinal radiation to the developing CNS; however, each case is evaluated independently with considerations for CSF dissemination or multifocal disease.

Prognosis.

The overall prognosis for ATRT is dismal, and a younger age at presentation corresponds to a worse prognosis. The mean survival for patients under 3 years of age is roughly 3-6 months; mean survival in older patients is roughly 12 months from the time of initial presentation.[30] There have been reports of curative treatment and survival measured in years, however, that is relatively uncommon and occurs more frequently in older patients.

Conclusion

CT and MRI are instrumental in the work-up, management, and follow-up of patients with primary posterior fossa brain tumors. Although imaging alone is insufficient to reliably predict histology prospectively, characteristic imaging features may help provide the most likely diagnosis, along with appropriate differential considerations. Therefore, it is essential that radiologists involved with interpretation of pediatric neuroimaging have a working knowledge of the imaging appearances associated with the most common pediatric posterior fossa brain tumors.

The views expressed in this material are those of the author, and do not reflect the official policy or position of the U.S. Government, the Department of Defense, or the Department of the Air Force.

References

1. Poretti A, Meoded A, Huisman TAGM. Neuroimaging of pediatric posterior fossa tumors including review of the literature. J Magn Reson Imaging 2012; 35: 32-47.
2. Davis FG, McCarthy BJ. Epidemiology of brain tumors. Curr Opin Neurol 2000; 13: 635–640.
3. Koeller KK, Rushing EJ. Medulloblastoma: a comprehensive review with radiologic-pathologic correlation. RadioGraphics 2003; 23: 1613-37.
4. Arseni C, Ciurea AV. Statistical survey of 276 cases of medulloblastoma (1935–1978). Acta Neurochir (Wien) 1981; 57: 159-162.
5. Farwell JR, Dohrmann GJ, Flannery JT. Central nervous system tumors in children. Cancer 1977; 40: 3123-3132.
6. Roberts RO, Lynch CF, Jones MP, Hart MN. Medulloblastoma: a population-based study of 532 cases. J Neuropathol Exp Neurol 1991; 50: 134–144.
7. Hubbard JL, Scheithauer BW, Kispert DB, et al. Adult cerebellar medulloblastomas: the pathologic, radiographic, and clinical disease spectrum. J Neurosurg 1989; 70:536–544.
8. Giordana MT, Schiffer P, Lanotte M, et al. Epidemiology of adult medulloblastoma. Int J Cancer 1999; 80: 689–692.
9. Eberhart CG, Kepner JL, Goldthwaite PT, et al. Histopathologic grading of medulloblastomas: a pediatric oncology group study. Cancer 2002; 94: 552–560.
10. Tortori-Donati P, Fondelli MP, Rossi A, et al. Medulloblastoma in children: CT and MRI findings. Neuroradiology 1996;38: 352 –359.
11. Nelson M, Diebler C, Forbes WSC. Paediatric medulloblastoma: atypical CT features at presentation in the SIOP II trial. Neuroradiology 1991; 33:140–142.
12. Koral K, Gargan L, Bowers DC, et al. Imaging characteristics of atypical teratoid-rhabdoid tumor in children compared with medulloblastoma. Am J Roentgenol 2008; 190: 809-14.
13. Jaremko JL, Jans LBO, Coleman LT, et al. Value and limitations of diffusion-weighted imaging in grading and diagnosis of pediatric posterior fossa tumors. Am J Neuroradiol 2010; 31: 1613-16.
14. Panigrahy A, Krieger MD, Gonzalez-Gomez I, et al. Quantitative short echo time 1H-MR spectroscopy of untreated pediatric brain tumors: preoperative diagnosis and characterization. Am J Neuroradiol 2006; 27: 560-72.
15. Kovanlikaya A, Panigrahy A, Krieger, et al. Untreated pediatric primitive neuroectodermal tumor in vivo: quantitation of taurine with MR spectroscopy. Radiology 2005; 236: 1020-25.
16. Massimino M, Cefalo G, Riva D, et al. Long-term results of combined preradiation chemotherapy and age-tailored radiotherapy doses for childhood medulloblastoma. J Neurooncol 2012; 108(1): 163-71.
17. Polkinghorn WR, Tarbell NJ. Medulloblastoma: tumorigenesis, current clinical paradigm, and efforts to improve risk stratification. Nat Clin Pract Oncol 2007; 4: 295-304.
18. Cohen BH, Zeltzer PM, Boyett JM, et al. Prognostic factors and treatment results for supratentorial primitive neuroectodermal tumors in children using radiation and chemotherapy: a Childrens Cancer Group randomized trial. J Clin Oncol 1995; 13(7): 1687-96.
19. Koeller KK, Rushing EJ. Pilocytic astrocytoma: radiologic-pathologic correlation. RadioGraphics 2004; 24: 1693-1708.
20. Jaremko JL, Jans LBO, Coleman LT, et al. Value and limitations of diffusion-weighted imaging in grading and diagnosis of pediatric posterior fossa tumors. Am J Neuroradiol 2012; 31: 1613-16.
21. Panigraphy A, Blüml S. Neuroimaging of pediatric brain tumors: from basic to advanced magnetic resonance imaging. J Child Neurol 2009; 24(11): 1343-65.
22. Mamelak AN, Prados MD, Obana WG, et al. Treatment options and prognosis for multicentric juvenile pilocytic astrocytoma. J Neurosurg 1994; 81:24–30.
23. Yuh EL, Barkovich AJ, Gupta N. Imaging of ependymomas: MRI and CT. Childs Nerv Syst 2009; 25: 1203-13.
24. Koeller KK, Sandberg GD. Cerebral intraventricular neoplasms: radiologic-pathologic correlation. RadioGraphics 2002; 22: 1473-1505.
25. Salazar OM. A better understanding of CNS seeding and a brighter outlook for postoperatively irradiated patients with ependymomas. Int J Radiat Oncol Biol Phys 1983; 9: 1231-1234.
26. Allen JC, Siffert J, Hukin J. Clinical manifestations of childhood ependymoma: a multitude of syndromes. Pediatr Neurosurg 1998; 28: 49-55.
27. Jallo GI, Biser-Rohrbaugh A, Freed D. Brainstem gliomas. Childs Nerv Syst 2004; 20: 143–153.
28. Poretti A, Meoded A, Huisman TAGM. Neuroimaging of pediatric posterior fossa tumors including review of the literature. J Magn Reson Imaging 2012; 35: 32-47.
29. Panigrahy A, Blüml S. Neuroimaging of pediatric brain tumors: from basic to advanced magnetic resonance imaging. J Child Neurol 2009; 24: 1343-65.
30. Burger PC, Yu IT, Tihan T, et al. Atypical teratoid/rhabdoid tumor of the central nervous system: a highly malignant tumor of infancy and childhood frequently mistaken for medulloblastoma: a Pediatric Oncology Group study. Am J Surg Pathol 1998; 22: 1083-1092.
31. Rorke LB, Packer RJ, Biegel JA. Central nervous system atypical teratoid/rhabdoid tumors of infancy and childhood: definition of an entity. J Neurosurg 1996; 85: 56-65.
32. Packer RJ, Biegel JA, Blaney S, et al. Atypical teratoid/rhabdoid tumor of the central nervous system: report on workshop. J Pediatr Hematol Oncol 2002; 24: 337-342.
33. Arslanoglu A, Aygun N, Tekhtani D, et al. Imaging findings of CNS atypical teratoid/rhabdoid tumors. Am J Neuroradiol 2004; 25: 476-80.
34. Koral K, Gargan L, Bowers DC, et al. Imaging characteristics of atypical teratoid-rhabdoid tumor in children compared with medulloblastoma. Am J Roentgenol 2008; 190: 809-14.
35. Hilden JM, Meerbaum S, Burger P, et al. Central nervous system atypical teratoid/rhabdoid tumor: results of therapy in children enrolled in a registry. J Clin Oncol 2004; 22: 2877-84.